Gene Duplication, Horizontal Gene Transfer, and Trait Trade-offs Drive Evolution of Post-Fire Resource Acquisition in Pyrophilous Fungi

Ehsan Sari[1], Dylan J. Enright[1], Maria Ordonez[1], Steven D. Allison[3], Peter M. Homyak[2], Michael J. Wilkins[4], Sydney I. Glassman[1*]

[1]Department of Microbiology and Plant Pathology, University of California, Riverside, CA, U.S.A.

[2]Department of Environmental Sciences, University of California, Riverside, CA, U.S.A.

[3]School of Biological Sciences, University of California, Irvine, CA, U.S.A.

[4]Department of Soil and Crop Sciences, Colorado State University, Fort Colins, CO, U.S.A

*Corresponding authors: sydneyg@ucr.edu and ehsans@ucr.edu

Author Contributions: S.I.G. designed the research, S.I.G, S.D.A., M.J.W. and P.M.H. acquired funding, E.S., D.J.E., and M.O. performed the culturing, molecular, and biophysical assays work. E.S. assembled and annotated fungal genomes, analyzed the data, and made figures. E.S. wrote the first draft of the paper with edits and contributions from all co-authors.

Competing Interest Statement: The authors declare no conflict of interest.

Classification: Major: Biological Sciences, **Minor:** Ecology

Keywords: Pyrophilous fungi, Comparative genomics, Aromatic carbon degradation, Nitrogen acquisition, Trait-trade-off

This PDF file includes:

Main Text

Figures 1 to 4

Abstract

Wildfires significantly alter soil carbon (C) and nitrogen (N), reducing microbial richness and biomass, while selecting for "fire-loving" pyrophilous microbes that drive post-fire nutrient cycling. However, the genomic strategies and functional trade-offs (balancing gains in one trait with costs in another) underlying the traits that enable pyrophilous microbes to survive and thrive post-fire are virtually unknown. We hypothesized that pyrophilous fungi employ specialized genomic adaptations for C and N cycling, with evolutionary trade-offs between traits governing aromatic C degradation, N acquisition pathways, and rapid growth. To test these hypotheses, we assessed hyphal extension rates and constructed a comparative genomics framework for 18 pyrophilous fungi from five Ascomycota (Eurotiales, Pleosporales, Sordariales, Coniochaetales, and Pezizales) and three Basidiomycota (Agaricales, Holtermaniales, and Geminibasidiales) orders isolated from burned soils. We found a dramatic trait trade-off between fast growth and number of genes responsible for aromatic C degradation, implying that these metabolically costly genes are selected for in burned environments despite their evolutionary cost. We used the comparative genomics framework to evaluate the genomic signatures of evolution and found that either gene duplication and somatic mutation, or recombination via sexual reproduction, were the primary drivers of fungal genomic variation in aromatic C degradation and N acquisition genes. Finally, we identified rare cross-kingdom bacterial to fungal horizontal gene transfer as a third strategy producing novel aromatic C degradation genes. Overall, we found that trait trade-offs and genome evolutionary strategies are key drivers of the rapid colonization and persistence of pyrophilous fungi in post-fire ecosystems.

Significance statement

Wildfires dramatically reshape soil ecosystems, yet the strategies that enable pyrophilous fungi to persist post-fire remain unclear. Here, we uncovered how pyrophilous microbes make evolutionary trade-offs like prioritizing aromatic C degradation at the expense of rapid growth to thrive post-fire. Our study is among the first to test theorized trait trade-off genomically and *in situ* across a wide fungal diversity. We identified cross-kingdom bacterial to fungal horizontal gene transfer, highlighting novel mechanisms of fungal genome evolution. We also identified patterns that can help predict microbial contributions to global C and N cycling. Finally, our findings highlight candidates that may be useful as fungal inoculants to enhance the recovery of burned soils or those polluted with other polycyclic aromatic hydrocarbons.

Introduction

Wildfires are increasing in intensity and severity (1), consuming nearly 3% of Earth's land surface (~464 M ha) every year (2), and altering the processes that govern the cycling and availability of carbon (C) and nitrogen (N) (3, 4). Wildfires also affect soil microbes (5, 6), altering their composition, function, and abundance. Fires reduce microbial richness and biomass, but they also promote specific taxa of pyrophilous "fire-loving" soil microbes (7), with uncertain effects on soil C and N cycling (4, 8). In particular, fires add complex charcoal-derived pyrogenic organic matter (PyOM) (9) and release high amounts of N (10), which pyrophilous microbes are critical to degrade. Despite these important biogeochemical roles, the genomic strategies and evolutionary trade-offs that enable pyrophilous fungi to survive and thrive post-fire are largely unknown.

Due to energetic costs and evolutionary constraints, trait trade-offs (balancing gains in one trait with costs in another) may limit fungal adaptation to post-fire biogeochemistry. Investment in certain traits,

such as rapid growth or thermotolerance, could limit resource allocation to other functions like nutrient acquisition (11–13). Drawing from plant ecological theory and Grime's C-S-R (Competitor-Stress tolerator-Ruderal) model (14), we previously proposed that pyrophilous microbes either excel at acquisition of post-fire resources such as high N or aromatic C in PyOM (competitors), thermotolerance (stress tolerators), or rapid growth in absence of competitors (ruderals) (12, 15). Investigating trait trade-offs provides insight into how fungi balance metabolic costs with ecological demands, which can result in a valuable framework for understanding and predicting microbial diversity and functions (11). Yet, empirical tests of these hypotheses remain scarce in microbial ecology. Trade-offs between stress tolerance, fast-growth, and C acquisition traits have been demonstrated in wood decaying fungi (16, 17), but not in other groups. *In situ* tests on cultures are a key step to determine whether these hypothesized trade-offs exist in pyrophilous fungi, with important implications for predicting global C and N cycling as fires continue to influence large tracts of the terrestrial biosphere.

Comparative genomics offers an unprecedented opportunity to gain insights into the genomic evolution and adaptations of pyrophilous fungi. Fungal genomes evolve through several mechanisms, including gene duplication, polyploidy, sexual reproduction, horizontal gene transfer (HGT), and transposable elements (TEs), all of which contribute to their functional and ecological diversity (18). Further, the unique prominent dikaryotic phase in Basidiomycota can lead to genomic novelty (19). Previous comparative analyses on several mushroom forming taxa from Pezizales and Agaricales have revealed unique genomic signatures in pyrophilous fungi, notably, expansions in gene families related to stress response, carbohydrate metabolism, and secondary metabolite biosynthesis (20, 21). Yet, further research is needed to generalize to completely microscopic fungi and to address potential trade-offs between fire-adaptive traits and other ecological or physiological characteristics.

We hypothesize that four key mechanisms–trait trade-offs, gene duplication, sexual recombination, and HGT–have driven the development of fire-associated traits in pyrophilous fungi. Trait trade-offs may have shaped fungal specialization, balancing investments in rapid growth, thermotolerance, and resource acquisition to maximize fitness in fire-disturbed ecosystems. Gene duplication combined with mutations, which is a major source of adaptation in fungi (22), likely plays a central role by expanding enzymatic gene families involved in PyOM degradation and N acquisition, enhancing metabolic versatility in post-fire environments. HGT, which can expand capacity and adaptation (23), may contribute to the acquisition of novel aromatic C degradation and N acquisition genes, enabling more efficient resource utilization and providing a competitive advantage in nutrient-limited post-fire soils. Finally, recombination during sexual reproduction could further increase genetic diversity by creating new combinations of alleles that optimize fungal responses to nutrient pulses and environmental stressors.

Here, we leveraged a large and diverse culture collection of pyrophilous fungi isolated primarily from post-fire mushrooms and soils across California (24) to identify genomic traits and trade-offs driving rapid post-fire colonization and persistence. We combined an *in-situ* growth assay with comparative genomics based on high quality, contiguous genomes of 18 pyrophilous fungi from orders of five Ascomycota and three Basidiomycota and found a dramatic trade-off between fast growth and the enrichment for genes encoding aromatic C degradation. Overall, we propose two major genome evolution strategies that underlie the pyrophilous fungal adaptation to post-wildfire environments: one relying on gene duplication and somatic mutation (e.g., in Eurotiales) and the other on sexual recombination (e.g., in Pezizales and Agaricales). Excitingly, we identified putative cross-kingdom horizontal gene transfer from bacteria to fungi as a rarer third strategy (e.g., in Coniochaetales and

Eurotiales) to enhance genetic diversity beyond the constraints of the gene pool. By generating new high-quality reference genomes for seven pyrophilous fungi, we advance understanding of fungal genome evolution in general as well as expand existing genomic research on pyrophilous fungi from two (20, 21) to eight fungal orders. Our findings support the hypothesis that trait trade-offs shape ecological function, with implications for global C and N cycling, and for creating microbial inoculants capable of breaking down polycyclic aromatic hydrocarbons that pollute many environments including burned soils.

Results

Genome assembly and gene annotation statistics: We generated 18 high-quality, contiguous fungal genomes from five Ascomycota orders (Coniochaetales, Eurotiales, Pezizales, Pleosporales, Sordariales) and three Basidiomycota orders (Agaricales, Geminibasidiales, Holtermanniales), which are all abundant in post-fire environments across a variety of fire-prone ecosystems (12, 15, 25), primarily from cultures isolated from burned soils and mushrooms following California wildfires (Table S1). We obtained 6.5-213 Gb of PacBio HiFi sequencing per genome with read N50 ranging from 5,429-10,028 bp providing 21-521X genome coverage (Table S2). Genome sizes ranged from 16.6 to 61.6 Mb, from 7 to 49 contigs, and contig N50 of 1.1 to 9.2 Mb (Table S3). We also assembled 21 to 267 Kb sized mitochondrial genomes with most isolates in a single contig (Table S4). Gene annotation guided by 2-15 million RNA-Seq paired-end reads per isolate enabled the identification 7,097-16,135 protein-coding genes per genome (Table S5). We sequenced the first genomes for 11 of our fungal isolates, with 6 providing completely novel reference genomes (Table S3, Figs. S1, S2). Finally, we improved upon previous genomes for 7 isolates (20, 21, 26) with most having fewer contigs, higher N50, and higher BUSCO scores (Table S6).

Trade-off between aromatic C degradation gene composition and fast growth: We paired genomes with biophysical assays to test if enrichment of aromatic C degradation and N acquisition genes trade off with growth on Malt Yeast Extract Agar (MYA) and PyOM media made from wildfire charcoal. We observed large variations in the enrichment of aromatic C degradation and N acquisition genes among pyrophilous fungal orders where Eurotiales had the most genes, followed by Pleosporales, then Coniochaetales and the lowest in Sordariales, Pezizales and Agaricales (Results S2; Fig. S3). We found that in general the Sordariales and Pezizales had the fastest growth whereas Eurotiales had the slowest growth (Fig. 1A), with a significant positive correlation between hyphal extension (HE) on MYA and PyOM media ($r=0.82$, $P=0.0001$; Fig. 1B). There was a dramatic trade-off between fast growth and enrichment of post-fire resource acquisition genes as indicated by strong, significant negative correlations ($r=0.53$-0.78, $P=0.0001$-0.05) between MYA or PyOM HE rates and the number orthologues of most aromatic C degradation genes (Fig. 1B). The microbial pathways involved in the decomposition of aromatic C in PyOM primarily include naphthalene degradation, catechol meta- and ortho-cleavage, and protocatechuate meta- and ortho-cleavage (27–29). Fungi transform aromatic C into intermediates such as catechol, protocatechuate, and benzoyl-CoA, followed by conversion to secondary intermediates such as acetyl-CoA, succinyl-CoA, and pyruvate through the bKA pathway (30). Interestingly, the number of *pcaF* orthologues from the bKA pathway, *mhpD* from the catechol metacleavage pathway, and *catB* from the catechol orthocleavage pathway were negatively correlated solely with HE on PyOM media. Contrary to our hypothesis, the correlation between N acquisition orthologue number and HE on both media types was insignificant (Fig. 1B).

Role of gene duplication in aromatic C degradation and N acquisition orthologues enrichment: We performed comparative genomic analysis using Orthofinder by adding 38 genomes of sister species with

158 publicly available genomes to 16 pyrophilous isolates within six fungal orders (Table S7). We excluded
159 Geminibasidiales (*Basidioascus undulatus*) and Holtermanniales (*Holtermanniella festucosa*) since they
160 are the only genomes sequenced from those orders. We tested the contribution of gene duplication to
161 gene enrichment by mining the Orthofinder output of the 54 genomes for the composition of 18
162 aromatic C degradation and 4 N acquisition orthologues (Table S8). Orthofinder partitioned duplication
163 events to the current species (pyrophilous and their sister species) and their common ancestors (named
164 arbitrarily by Orthofinder as N0-N51) in the species tree, providing insights into the duplication event
165 history during evolution. We inferred two distinct groups at the N2 common ancestor. The first group,
166 containing the Eurotiales, Pleosporales, Sordariales, and Coniochaetales, had more aromatic C
167 degradation orthologues, while the second group with Pezizales and Agaricales had fewer orthologues
168 (Fig. 2). To test if more than one major duplication event led to the enrichment seen in the first group,
169 we compared the common ancestors descended from N2. We found that the duplication rate at N6–the
170 ancestor of Eurotiales, Pleosporales, Sordariales, and Coniochaetales–was 4X higher than at the
171 concurrent node N5, which also descends from N2 and gave rise to the Pezizales and Agaricales.
172 Meanwhile, N11 containing Sordariales and Coniochaetales, experienced a decline in duplication events,
173 while N10 containing the Eurotiales and Pleosporales, and N18, the common ancestor of all
174 contemporary Eurotiales maintained large duplication events. Within Eurotiales, the common ancestor
175 of *Penicillium* at N36 had 10X higher duplication than the common ancestor of *Aspergillus* at N37.

176 **HGT involved in the higher enrichment of *catA*:** Considering the phylogenomic relatedness of orders
177 and reduced duplications events at N11 (Fig. 2), we expected both Coniochaetales and Sordariales to
178 convergently evolve to lower number of aromatic C degradation and N acquisition orthologues than
179 Eurotiales and Pleosporales. However, Coniochaetales species had notably more orthologues like
180 catechol-1,2-dioxygenase (*catA*) from the bKA pathway than Sordariales, suggesting that gene
181 duplication is not the only cause of aromatic C degradation and N acquisition orthologue enrichment.

182 We used multiple methods to test for HGT. First, we examined the gene trees of *catA* orthologues and
183 identified OG0001245, an orthogroup carrying 63 *catA* orthologues. This lent support for HGT in the
184 pyrophilous species *Coniochaeta hoffmannii*, *Penicillium atrosanguineum*, and *Rasamsonia columbiensis*
185 (Fig. 3A), since each had two paralogues of *catA*, one of which clustered distantly from the orthologues
186 of their sister taxa. Gene CH_06113.t1 from *C. hoffmannii* was clustered distantly from its paralogue
187 CH_10993.t1, and close to an orthologue from *P. atrosanguineum* (PR_10622.t1). Gene PR_10622.t1
188 from *P. atrosanguineum* was clustered distantly from all the other Eurotiales orthologues including its
189 paralogue PR_04517.t1. Gene RC_00189.t1 formed a distinct cluster with an orthologue from *R.*
190 *emersonii* (XP_013325789.1) close to the Pezizales orthologues, while its paralogue RC_0097.t1 was
191 clustered with the other Eurotiales orthologues. Due to the lack of identity by descent, we propose that
192 CH_06113.t1, PR_10622.t1, and RC_00189.t1 were introduced through HGT.

193 Second, we used multiple sequence alignment to align the protein sequences of the three HGT
194 candidates and their native paralogues, and the resulting phylogenetic tree supported the distinction
195 between the HGT candidates and their native paralogues (Fig. S4). We found a large deletion in
196 CH_06113.t1, making it distinct from all the other five proteins (i.e., its native paralogue CH_10933.t1).

197 Third, since previous research indicated that HGT introduced genes had lower transcription than their
198 native counterparts (31), we examined their transcription levels and found that all three candidate HGT
199 genes had lower transcripts per million (TPM) values than their native counterparts (Fig. 3B). Fourth,

since previous research suggested that HGT genes accumulate higher nucleotide polymorphisms than their native paralogues (32), using variation in sister taxa orthologues as a baseline for comparison, we found higher numbers of nucleotide polymorphisms between orthologues of sister taxa and HGT candidates than their native paralogues (Fig. 3C). The difference was often larger for non-synonymous nucleotide polymorphisms (polymorphisms leading to protein amino acid changes).

Finally, we further examined the possibility of cross-kingdom HGT from bacteria to fungi. We found a Ty3-line (Gypsy) Long Terminal Repeat (LTR) retrotransposon of ~18 kb spanning CH_06113.t1 and the two neighboring genes (Fig. S5). The BLAST search against the Swiss-Prot database described CH_06113.t1 as "similar to hqdA Intradiol ring-cleavage dioxygenase hqdA (*Aspergillus niger*)", and one of the neighboring genes as "similar to tftE Maleylacetate reductase (*Burkholderia cepacia*)". When the protein sequence of CH_06113.t1 was used as an inquiry for NCBI BLASTP search against prokaryotes gene bank, we found several orthologues. We retrieved the protein sequences of the top 20 blast hits based on the percentages of sequence identity and query coverage and combined with the protein sequences of 20 fungal orthologues for phylogenetic analysis, revealing that the bacterial orthologues formed a distinct cluster from those of fungi in the phylogenetic tree, suggesting an ancient cross-kingdom HGT (Fig. S6).

Role of sexual reproduction in high variation in aromatic C and N acquisition genes: We tested if sexual recombination contributed to the genetic variation in aromatic C and N acquisition genes in pyrophilous fungi. We examined synonymous (S) and nonsynonymous (NS) nucleotide substitution rates separately to distinguish neutral mutation rates from adaptive selection pressures to determine whether variation in the nutrient acquisition pathways arose from selection for metabolic specialization (e.g., in aromatic C degradation) or neutral diversification processes. To facilitate the visualization of results, we selected one orthogroup from each of the examined pathways (Table S8).

Eurotiales had consistently high numbers of S and NS substitutions across all pathways (Fig. 4). Pezizales species exhibited comparable and sometimes higher S and NS substitutions than Eurotiales, despite having remarkably lower gene duplication events (Figs. 2; S3). Two Pezizales isolates, *Peziza echinospora* and *Geopyxis carbonaria*, ranked highest in the substitution number of the catechol metacleavage and naphthalene degradation orthogroups (Fig. 4).

To distinguish pyrophilous adaptations from phylogenetic relatedness, we compared pyrophilous fungi and their non-pyrophilous sister taxa and found that some pyrophilous fungi exhibited higher genetic variation in aromatic c degradation genes than their sister taxa. *Aspergillus cf. felis* had notably higher substitutions in the catechol orthocleavage, catechol metacleavage, bKA pathway, and naphthalene degradation orthogroups than all the other sister *Aspergillus* species, and *Alternaria* sp. had higher substitutions in the catechol orthocleavage orthogroup than all the other *Alternaria* species (Fig. 4). *Coniochaeta hoffmannii* had the highest NS substitutions in the bKA pathway orthogroups within the Coniochaetales and also ranked top among all 53 taxa. Within Pezizales, *Peziza echinospora* had the highest NS substitutions in the bKA pathway and naphthalene degradation orthogroups.

Dikaryotic internuclear variation contributes to nitrate-reductase (narG-narZ) variation: The dominant dikaryotic phase common in Basidiomycota where two genomes exist in two separate nuclei in each cell allows them to take advantage of diploid genomes (e.g., increased genetic diversity and protection against deleterious mutations) while reducing the tension between unrelated haploid genomes (33). We leveraged our high-quality assemblies to establish phased genomes to test the contribution of

242 internuclear variation to higher genetic variation observed in nitrate-reductase (*narG-narZ*) genes within
243 Agaricales (Fig. 4). We found a high number of substitutions in the Agaricales OG0000632 orthogroup
244 described as *narG-narZ*. We selected an OG0000632 orthologue of *Lyophyllum atratum* (LA_01440.t1)
245 and aligned two haplotypes representing the sequences of two nuclei and found 16 nucleotide
246 polymorphism sites in the exonic regions (Fig. S7). We then aligned RNA-seq reads to one haplotype as a
247 reference and observed reads derived from both haplotypes at a nearly 1:1 ratio at all 16 polymorphism
248 sites, indicating that the two haplotypes were transcribed in equilibrium. This suggests that internuclear
249 variation drove the higher number of substitutions in *narG-narZ* in *L. atratum*.

250 **Discussion**

251 We provided an *in-situ* test of often hypothesized but rarely tested ecological theory to reveal a
252 fundamental trait trade-off between ability to grow fast or break down aromatic hydrocarbons in
253 pyrophilous fungi. This genomic balancing act underpins the selective advantage of carrying larger suites
254 of aromatic C degradation genes in wildfire-impacted environments. Our findings suggest that gene
255 duplication and mutations represent one route for generating genetic variation within aromatic C
256 degradation and N acquisition genes in pyrophilous fungi (e.g., in Eurotiales), while recombination via
257 sexual reproduction and internuclear variation offer an alternative mechanism (e.g., in Pezizales and
258 Agaricales). Finally, we show evidence that ancient bacterial to fungal cross-kingdom HGT contributes to
259 genetic novelty in PyOM degradation in pyrophilous fungi (e.g., in Coniochaetales and Eurotiales). Our
260 research expands our understanding of the contribution of genome evolution to fungal adaptation to
261 post-fire environments by integrating comparative genomics and growth assays to link specific genetic
262 changes with ecological outcomes, and highlights overlooked fungal lineages with exceptional potential
263 for aiding ecosystem recovery after disturbances.

264 **Microbial trait trade-offs at genomic levels:** Combining hyphal extension assays with high-quality
265 genomes of 16 filamentous pyrophilous fungal isolates, we found large, significant trade-offs between
266 fast growth and enrichment for aromatic C degradation genes. This was epitomized by the Ascomycota
267 orders Pezizales, which grew fast at the expense of fewer aromatic C breakdown orthologues, and
268 Eurotiales, which grew slowest but was enriched for aromatic C degradation. Surprisingly, we found no
269 trade-offs between fast growth and enrichment of genes for N acquisition, which may reflect that
270 efficient N scavenging is a widespread evolutionary pressure across most ecosystems (34). In contrast,
271 the recalcitrance of PyOM requires highly specialized enzymatic machinery (35), creating a stronger
272 metabolic cost driving the trade-off with growth. The fast-growth-aromatic C acquisition trade-off
273 observed here, along with genetic and copy number variation within the aromatic C degradation and N
274 acquisition orthologues, supports the ideas of functional diversity and specialization among pyrophilous
275 fungal lineages. The rapid growth of Pezizales species corresponds to their early successional role in
276 post-fire environments, coinciding with a surge of bioavailable nutrients from necromass (15, 36).
277 Similarly, the comparatively slower growth of Eurotiales aligns with their late successional role, where
278 enrichment of aromatic C-degrading genes likely facilitates resource acquisition from difficult to degrade
279 PyOM (37). Many Eurotiales are known for their rapid colonization of various substrates (38), which
280 made their slower growth unexpected; however, it might be specific to the pyrophilous Eurotiales
281 species we examined, as evidenced by higher enrichment of aromatic C genes in pyrophilous Eurotiales
282 and their sister species than other Eurotiales. This variation in growth rates among Eurotiales highlights
283 the diverse ecological strategies within the order, ranging from fast-growing opportunists to more
284 specialized, slower-growing species adapted to specific niches like post-fire environments.

New pyrophilous taxa as candidate contributors to aromatic C degradation and N acquisition: Our results suggest that three Ascomycota orders–Eurotiales, Pleosporales, and Coniochaetales–are likely major players in aromatic C degradation due to higher gene enrichment. We know of only two prior studies examining pyrophilous fungal genomes, which focused on six isolates of Pezizales and three of Agaricales that all formed mushrooms on burnt soil (20, 21). In contrast, Eurotiales, Pleosporales, and Coniochaetales do not form macroscopic fruiting bodies but are commonly identified in microbiome studies of burned soils (12, 15, 25) and we isolated them from burnt soil slurries (24). The Eurotiales isolates we studied included *Rasamsonia columbiensis,* which is a thermotolerant species (38) that has been isolated from house dust (39), *Penicillium atrosanguineum* which has been isolated from forest soil (40), *P. antarcticum*, which was previously isolated as an endophyte from Antarctica native plants (41), and *Aspergillus fellis,* also previously isolated as an endophyte (42) and from rocks (43). Endophytic fungi may be potent decomposers of aromatic C due to their ability to decompose the host's dead cell wall and penetrate host plant barriers while establishing endophytic relationships (44). The endophytic lifestyle could be linked with post-fire survival by providing an escape mechanism, as internal colonization of plant tissues especially roots offer insulation from extreme heat and flames, allowing fungi to persist and subsequently colonize burned soil (45, 46). Pleosporales, such as *Alternaria*, are adapted to a wide range of ecological niches and are ubiquitous saprobes, wide-host-range plant pathogens, and plant endophytes (47). *Coniochaeta hoffmannii* is also known as a wood-decaying soil fungus and a plant pathogen that was previously isolated from a car fuel reservoir and can degrade polypropylene plastic (48). Eurotiales, Coniochaetales, and Pleosporales pyrophilous species, characterized by enriched aromatic C degradation and N acquisition genes and extremophilic adaptations to environments like Antarctic soils, fuel reservoirs, and pyrolyzed substrates, exhibit dual capacities critical to post-wildfire recovery, i.e., degradation of fire-derived aromatics (e.g., polypropylene-like pyrolyzed compounds), and tolerance of post-fire abiotic stressors (e.g., desiccation and UV exposure). Their genomic toolkit, refined through adaptation to harsh niches, positions these fungi as key mediators of C and N cycling in burned soils, with potential applications in restoring fire-disturbed ecosystems. In contrast, the Basidiomycete pyrophilous fungi did not have as many genes for aromatic C degradation, which may reflect their specialization in lignin degradation (49).

We assembled contiguous genomes for two basidiomycete yeasts, *Holtermanniella festucosa* from Holtermanniales and *Basidioascus undulatus* from Geminibasidiales, which were both genomic orphan orders. These species are novel pyrophilous fungi and have been repeatedly identified in previous studies as dominant soil colonizers following wildfire (12, 15, 25, 50). However, due to the absence of closely related reference genomes, we were unable to include these isolates in our comparative genomic analyses. Future studies should prioritize sequencing additional species from these orders to enable investigation of the genetic mechanisms underlying pyrophilous traits and associated trait trade-offs.

Gene duplication, an adaptation strategy to post wildfire environments in pyrophilous fungi: Our study revealed that ancient gene duplication plays a crucial role in shaping the current composition of aromatic C degradation and N acquisition genes in pyrophilous fungi, likely as an adaptation to frequent exposures to post-wildfire environments. Gene duplication is a well-established mechanism for creating genetic variation and functional innovation across different forms of life and especially within Kingdom Fungi, where five large gene duplication bursts have been identified (51). Among our isolates, gene duplications decreased throughout evolutionary history, but this decline was slower for the common ancestors of the current pyrophilous species in the Eurotiales, Pleosporales, Sordariales, and

328 Coniochaetales orders. Eurotiales species showed the slowest decline, maintaining the largest repertoire
329 of aromatic C degradation genes in their contemporary forms. This slow decline leading to high load of
330 aromatic C degradation genes highlights the significant role that Eurotiales likely play in aromatic C
331 degradation, at least in fire disturbed chaparral soil, where our pyrophilous Eurotiales species were
332 isolated (24). A previous study found a correlation between gene copy numbers of ring-hydroxylating
333 dioxygenase in soil samples and degradation efficiency, highlighting the quantitative nature of microbial
334 aromatic C degradation (52). Gene duplication thus provides novel genes for higher expression and
335 functional diversification. While gene duplication affecting C and N metabolism is a common
336 evolutionary strategy in other fungi (22), our findings underscore its particular importance for
337 pyrophilous fungi, likely representing a specific adaptation to unique post-fire C and N resources.
338 However, we observed differential duplication frequencies between aromatic C and N acquisition genes
339 across pyrophilous fungal species, which suggests lineage-specific variations in employing gene
340 duplication as an adaptive strategy within fire-associated ecosystems.

341 **Enhancing genetic variation in aromatic C and N acquisition genes through ancient HGT:** Here, we
342 provide for the first time compelling evidence for an ancient HGT of a *catA* gene from bacteria to *C.*
343 *hoffmannii, R. columbiensis* and *P. atrosanguineum.* Our phylogenetic analyses using the *catA*
344 orthologues in fungi and bacteria suggested distinction between bacterial and fungal sequences, likely
345 due to an ancient HGT event subjected to distinct evolution trajectories in fungi. This is further
346 supported by the presence of *catA* HGT events in both Coniochaetales and Eurotiales. It is possible that
347 this gene was transferred into their common ancestor and subsequently lost in some descended taxa
348 possibly due to fitness penalties. HGT from bacteria to fungi is increasingly recognized as a significant
349 mechanism for fungal genome evolution and adaptation (53). Notable examples include the transfer of
350 bacterial glycosyl hydrolases to Neocallimastigomycota rumen fungi, enhancing their ability to break
351 down plant material (54). The HGT events in aromatic C degradation genes like *catA* may have conferred
352 a novel function allowing pyrophilous fungi to outperform native soil communities in acquiring C from
353 PyOM, which might be tested with future research generating a knockout of the HGT *catA* gene in
354 pyrophilous fungi like *C. hoffmannii*. The cross-kingdom HGT of aromatic C acquisition genes is a novel
355 mechanism of adaptation in pyrophilous fungi to post-fire environments, where higher genetic variation
356 in aromatic C degrading genes is likely advantageous.

357 **Contribution of sexual recombination versus gene duplication to pyrophilous fungal genetic variation:**
358 The number of nucleotide polymorphisms varied substantially across pyrophilous orders and surprisingly
359 did not linearly increase with the number of gene duplications. Pezizales exhibited comparable, and in
360 some cases, higher nucleotide polymorphisms than Eurotiales, despite having significantly fewer gene
361 copies. Differences in sexual reproduction frequency, which is rare among Eurotiales species, with some
362 reproducing strictly asexually (38), but common among pyrophilous Pezizales species (20), may suggest
363 two distinct mechanisms for maintaining diversity in pyrophilous fungi. In fungi with limited sexual
364 reproduction, like Eurotiales, genetic variation could be maintained through gene duplication followed
365 by somatic mutations. In contrast, genetic variation might balance through sexual recombination in
366 lineages like Pezizales with frequent sex and obvious fruiting bodies. The high genetic variation observed
367 in aromatic C degradation and N acquisition genes could allow pyrophilous Pezizales species such as
368 *Pyronema omphalodes* to access various bioavailable C and N resources released from necromass
369 immediately post fire, explaining the rapid colonization of burned soil by *Pyronema* (15, 36). The slower-
370 growing Eurotiales pyrophilous species appear to take over later in succession (15), likely due to their

371 higher gene copies which enable them to acquire more complex aromatic C and N resources that are
372 inaccessible to pyrophilous Pezizales. We also identified internuclear variation in *L. atratum*, a
373 Basidiomycete with a dominant dikaryotic phase, associated with a nitrate-reductase (*narG-narZ*) gene
374 that exhibited unexpectedly high genetic variation. This finding further supports the role of sexual
375 reproduction and dikaryon formation in Basidiomycota as a mechanism for enhancing genetic variation
376 in resource acquisition genes among pyrophilous fungi. Together, these results underscore distinct
377 evolutionary strategies employed by pyrophilous fungi to maintain genetic diversity and adapt to the
378 dynamic nutrient landscapes of post-fire environments.

379 **Conclusions:** Our study advances fungal genomics by expanding the genomic resources for pyrophilous
380 fungi, including several previously uncharacterized lineages. By conducting one of the first *in-situ* tests of
381 trait trade-offs in pyrophilous fungi using a large culture collection and high-quality genomes, we reveal
382 that pyrophilous fungi exhibit a striking trade-off between rapid growth and the enrichment of aromatic
383 C degradation genes, an adaptation that likely confers a selective advantage in fire-affected soils
384 dominated by PyOM. Our study suggests that at least two major genome evolution strategies manifest
385 the adaptation of pyrophilous fungi to post-wildfire environments: one relying on gene duplication and
386 somatic mutation (e.g., in Eurotiales) and the other on sexual recombination (e.g., in Pezizales and
387 Agaricales). Rare HGT events, as examined in *C. hoffmannii*, *R. columbiensis* and *P. atrosanguineum*, is
388 likely a third strategy enhancing genetic diversity in pyrophilous fungi beyond the gene pool barrier.
389 Future research should investigate how these distinct evolutionary strategies influence interactions
390 among pyrophilous fungi, prioritizing the study of newly identified species with enriched aromatic C and
391 N acquisition genes. Collectively, our findings not only expand the frontier of pyrophilous fungal
392 genomics but also provide a foundation for leveraging these microbes to accelerate post-fire ecosystem
393 recovery and nutrient cycling.

394 **Materials and Methods**

395 **Fungal isolates:** We leveraged our collection of pyrophilous fungi isolated primarily from post-fire
396 mushrooms and soils across California. We included 18 pyrophilous fungal isolates from across two phyla
397 and 8 orders (Table S1). We selected these isolates because they were abundant across a variety of fire-
398 prone ecosystems (7, 12, 15, 25) and we expected them to exhibit a diversity of pyrophilous trait
399 strategies (12).

400 **High Molecular Weight (HMW) DNA Extraction and PacBio HiFi Sequencing:** We extracted HMW DNA
401 from fungal tissue with either Qiagen Genomic Tip 100/G (Qiagen, Hilden, Germany) or using a
402 CTAB:Phenol:Chloroform method (55) if extraction with Qiagen Tips led to low DNA concentration (Table
403 S1). See Methods S1 for fungal tissue preparation and DNA extraction details.

404 We then submitted DNA to the University of California Irvine Genomics Research and Technology Hub
405 (UCI GRTH) for HiFi SMRT Bell Library Preparation and PacBio HiFi Sequencing. The sequencing library
406 was prepared using SMRTbell template prep kit version 3.0 with the overhang barcoded adapters
407 (PacBio, Menlo Park, USA) and sequenced on the Sequel IIe™ System (PacBio, Menlo Park, USA), except
408 for *Neurospora sp.* E-DF1, *Neurospora discreta* E-DF3, and *Tricharina praecox*, which were sequenced
409 using the Revio™ system (PacBio, Menlo Park, USA). Samples were multiplexed to achieve the genome
410 coverage ≥ 20X.

411 **Genome Assembly Pipeline:** We generated draft genome assemblies for each isolate using Hifiasm
412 v.0.16.1-r375 (56), IPA v.1.8.0 (https://github.com/PacificBiosciences/pbipa), hiCanu v.2.2 (57), Peregrine
413 v.0.4.13 (https://github.com/cschin/peregrine-2021?tab=readme-ov-file), and Flye v.2.9-b1774 (58). We
414 obtained the assembly metrics using QUAST software v.5.2.0 (59), and used BUSCO software v.5.4.3 to
415 assess assembly completeness (60). We used the most contiguous and complete assembly as a reference
416 for scaffolding with the Masurca software v.4.1.0 SAMBA tool (61) with raw HiFi reads and then with the
417 other inferior draft assemblies as inputs. We identified and corrected the miss-assemblies using CRAQ
418 software v.1.0.9 (https://github.com/JiaoLaboratory/CRAQ). We found telomere repeat sequences with
419 the FindTelomeres script (https://github.com/JanaSperschneider/FindTelomeres). We assembled the
420 mitochondrial genome using get_organel software v.1.7.7.1
421 (https://github.com/Kinggerm/GetOrganelle) with the Hifiasm assembly graph as an input.

422 **RNA extraction and sequencing:** We grew the 18 fungal isolates in three conditions: in malt yeast broth
423 1) at ambient temperature 2) in ambient temperature followed by a 1 hr 40 °C heat-shock, or 3) on
424 PyOM agar plates covered with cellophane sheets at ambient temperature. We extracted total RNA with
425 the E.Z.N.A.® Fungal RNA Mini Kit (Omega Bio-Tek, Norcross, U.S.A.) following manufacturer's protocol.
426 See Methods S2 for method used for the RNA quality control. We prepared mRNA Illumina libraries using
427 the Illumina TruSeq® RNA Sample Preparation v. 2 Kit (Illumina, San Diego, USA) and sequenced on the
428 NovaSeq 6000 system (Illumina, San Diego, USA) at the UCI GTRH.

429 **Gene and TE Annotation**: We used RNA-seq data to annotate the protein-coding genes with the FunGAP
430 pipeline (62) after trimming sequencing adapters with TrimGalore v.0.6.10
431 (https://github.com/FelixKrueger/TrimGalore), and filtering to retain only reads with a Phred quality
432 score > 30 and length of ≥ 50 bp. We assigned putative sequence descriptions to protein sequences
433 predicted by FunGAP by searching with NCBI-BLASTP v.2.16.0 (https://blast.ncbi.nlm.nih.gov) against the
434 reviewed UniProtKB database (Swiss-Prot, downloaded in Aug 2023). For each protein, we extracted the
435 InterPro protein families and Gene Ontology (GO) terms (63) using InterProScan v. 5.62-94.0
436 (https://interproscan-docs.readthedocs.io/en/latest/) and the Kyoto Encyclopedia of Genes and
437 Genomes (KEGG) ontology terms using kofam_scan v.1.3.0 (https://github.com/takaram/kofam_scan).
438 We annotated the mitochondrial genes with the GeSeq online tool (https://chlorobox.mpimp-
439 golm.mpg.de/geseq.html). We annotated TEs with the Transposon Annotator "reasonaTE" tool (64) and
440 calculated the percentage of the genome annotated as TEs by dividing the number of nucleotides in the
441 annotated TE regions by the total genome length, multiplied by 100.

442 **Annotation of Aromatic C Degradation and N-acquisition Genes:** We generated Hidden Markov Model
443 (HMM) profiles for 18 aromatic C degradation and 4 N acquisition genes (Table S8) examined previously
444 (28). Aromatic C degradation genes examined belonged to meta- and ortho-cleavage for both catechol
445 and protocatechuate and naphthalene degradation pathways (27–29). According to previous studies,
446 fungi transform aromatic C into intermediates such as catechol, protocatechuate, and benzoyl-CoA,
447 followed by conversion to secondary intermediates such as acetyl-CoA, succinyl-CoA, and pyruvate
448 through the β-ketoadipate (βKA) pathway (30), so we also examined genes from the bKA pathway.

449 We also examined N acquisition genes such as nitrate and nitrite reductase whose transcription were
450 previously shown to increase after fire (65). We also included nitrous oxide reductase (*nosZ*) since high-
451 severity fires may impair the soil microbiome's capacity to convert nitrous oxide (N_2O), a potent GHG, to
452 nitrogen (N_2) gas (66), leading to elevated N_2O emission from burnt soil (67). Fungi play a unique role in

453 this process. We also included *P450nor* because some fungi possess Cytochrome P450 nitric oxide
454 reductase (*P450nor*), an enzyme that catalyzes the reduction of nitric oxide (NO) to N_2O during fungal
455 denitrification (68).

456 We downloaded all protein sequences associated with each gene from NCBI, and discarded proteins
457 annotated as similar or partial in their FASTA headers. We then aligned the high-confidence protein
458 sequences of each gene using ClustalOmega v. 1.2.4 (69) with default parameters and used the
459 alignments to build HMM profiles using the hmmbuild command of HMMER v.3.4 (http://hmmer.org/).
460 We used these HMM profiles to annotate each fungal isolate's protein sequences using the hmmsearch
461 command of HMMER v.3.4, with an E-value cutoff of 1e-23. To confirm that the hmmsearch accurately
462 retrieved the orthologues of each gene, we matched the available sequence descriptions and domain
463 annotations obtained using BLAST and Interproscan with the description of proteins used as inputs for
464 building HMM profiles.

465 **Orthogroup Construction and Visualization:** We performed comparative genomic analysis of 16
466 pyrophilous fungi of the 6 orders along with 38 sister species (Table S7) selected as described in Methods
467 S3. We assigned genes to orthogroups (clusters of orthologues across genomes) using Orthofinder
468 v.2.5.5 (70) and used the gene IDs of HMMER annotated aromatic C degradation and N acquisition genes
469 to extract assigned orthogroups from the Phylogenetic Hierarchical Orthogroups predicted for the oldest
470 common ancestor of all species (N0). We obtained the orthogroups per gene family and individual genes
471 by creating a matrix of orthologue counts per species. We visualized the sum of genes for each of
472 naphthalene degradation, catechol meta- and ortho-cleavage, protocatechuate (PCA) ortho- and meta-
473 cleavage, and N-acquisition pathways alongside the species tree generated with Orthofinder using the
474 plotTree.barplot function of Phytools (https://cran.r-project.org/web/packages/phytools/index.html) in
475 R v.4.3.2 (71). To identify gene duplication events leading to the current composition of aromatic C
476 degradation and N acquisition genes in the pyrophilous fungi, we obtained the number of gene
477 duplication events in these genes occurring at each current node (53 species) and their common
478 ancestors from the Orthofinder Gene Duplication Events reports. We visualized the number of gene
479 duplication events on the phylogenetic tree alongside the orthologue counts per individual gene using
480 iTOL software v.7 (https://itol.embl.de/).

481 **Identification of candidate HGT events:** We identified candidates for HGT events by visually inspecting
482 the putative xenologues generated by Orthofinder for outlier orthologues clustered distantly from their
483 sister species in their gene trees then validated them with the following steps. We visualized the aligned
484 protein sequences of candidate HGT genes and their corresponding native genes in the orthogroup using
485 iTOL software v.7 (https://itol.embl.de/). Next, we compared candidate HGT gene transcription levels
486 with their corresponding native genes (orthologues complying with phylogeny in the gene tree) in the
487 orthogroup. We aligned the RNA-seq reads to their corresponding fungal genome using HISAT2 v.2.2.1
488 (72). We then calculated the Transcript Per Million (TPM) values for each gene using TPMCalculator
489 v.0.0.5 (73) from the spliced alignment BAM file generated with HISAT2. Next, we calculated synonymous
490 (S) and non-synonymous (NS) nucleotide substitution rates of the HGT candidates and their
491 corresponding native genes using KaKs_Calculator v.3.0 (74). We also examined the co-localizations of
492 the loci with the candidate HGT genes and TEs by visualizing the GFF3 files containing gene and TEs
493 annotations in Integrated Genome Viewer (IGV) software v.2.15.2 (75). Finally, we BLASTed the protein
494 sequences of candidate HGT genes against all deposited proteins from other kingdoms (i.e., bacteria,

plants, and animals) to identify potential donor species using BLASTP v.2.16.0 (https://blast.ncbi.nlm.nih.gov/Blast.cgi).

Measuring genetic variation among taxa in aromatic C degradation and N acquisition genes: We calculated the nucleotide substitution rate of the aromatic C degradation and N acquisition genes for the 53 genomes subjected to orthogroup construction with KaKs_Calculator v.3.0 (74). We visualized with a heatmap generated for a single orthogroup per each of the naphthalene degradation, catechol meta and ortho-cleavage, and protocatechuate meta and ortho-cleavage, and N acquisition pathways using the heatmap.2 function of R v.4.3.2 (76). See Methods S4 for methods examining contribution of internuclear variation in Basidiomycota to variation among aromatic C degradation and N acquisition genes.

Measuring trade-off between fast-growth, and aromatic C degradation and N-acquisition: We measured HE rate on MYA or PyOM media for 16 filamentous pyrophilous isolates using three biological replicate plates per media type per isolate. We covered each plate with a sterile cellophane sheet (16), then inoculated a 5 mm^2 radius plugs of fungal tissue into the center, then incubated at room temperature with the hyphal growing edge recorded every 24 h using alternating-colored markers. After 3 weeks, plates were photographed, and images were imported into ImageJ v.1.54 (https://imagej.net/ij/) where daily extension rates were quantified in millimeters per day. We calculated the pairwise Spearman's rank correlation between the HE rates on MYA and PyOM media and the number of each aromatic C degradation and N acquisition orthologues of each species using the rcorr function (77) and visualized using the corrplot function of R (78).

Acknowledgements: This project was funded by the Department of Energy BER Award #DE-SC0023127 to SIG, PMH, SDA, and MJW and United States Department of Agriculture-NIFA Award #2022-67014-36675 to SIG and PMH. We thank many individuals who contributed to the Glassman lab pyrophilous microbial culture including lab managers Judy Chung and James Randolph, lab assistants Ryan Quaal and Aishwarya Veerabahu, collaborators Tom Bruns and Monika Fischer, UCR PhD students Fabiola Pulido-Chavez, Arik Joukhajian, Esbeiry Cordova-Ortiz, and Mark Yacoub, and UCR undergraduates Anna Nguyen, Marely Vega, Jenna Maddox, Justin Diab, Wine-Jie Lipardo, Audrey Reichard, Priscilla Shultz, Jorge Ponce, and Nathan Heger. We thank Jason Stajich and his lab for advice and protocols for high molecular weight DNA extraction. We thank our anonymous reviewers for their helpful feedback on the manuscript.

References

1. C. X. Cunningham, G. J. Williamson, D. M. J. S. Bowman, Increasing frequency and intensity of the most extreme wildfires on Earth. Nat Ecol Evol 8, 1420–1425 (2024).

2. J. T. Randerson, Y. Chen, G. R. Van Der Werf, B. M. Rogers, D. C. Morton, Global burned area and biomass burning emissions from small fires. J Geophys Res Biogeosci 117, G04012 (2012).

3. D. G. Neary, C. C. Klopatek, L. F. DeBano, P. F. Ffolliott, Fire effects on belowground sustainability: a review and synthesis. For Ecol Manage 122, 51–71 (1999).

4. L. E. Nave, E. D. Vance, C. W. Swanston, P. S. Curtis, Fire effects on temperate forest soil C and N storage. Ecological Appl 21, 1189–1201 (2011).

5. S. R. Dooley, K. K. Treseder, The effect of fire on microbial biomass: A meta-analysis of field studies. Biogeochemistry 109, 49–61 (2012).

6. Y. Pressler, J. C. Moore, M. F. Cotrufo, Belowground community responses to fire: meta-analysis reveals contrasting responses of soil microorganisms and mesofauna. Oikos 128, 309–327 (2019).

7. S. Fox, et al., Fire as a driver of fungal diversity — A synthesis of current knowledge. Mycologia 114, 215–241 (2022).

8. B. M. Goodridge, et al., Retention of nitrogen following wildfire in a chaparral ecosystem. Ecosystems 21, 1608–1622 (2018).

9. C. Santín, S. H. Doerr, C. M. Preston, G. González-Rodríguez, Pyrogenic organic matter production from wildfires: a missing sink in the global carbon cycle. Glob Chang Biol 21, 1621–1633 (2015).

10. P. C. Campbell, et al., Pronounced increases in nitrogen emissions and deposition due to the historic 2020 wildfires in the western U.S. Sci of The Total Environ 839, 156130 (2022).

11. A. A. Malik, et al., Bacterial population-level trade-offs between drought tolerance and resource acquisition traits impact decomposition. ISME J 18, 224 (2024).

12. D. J. Enright, K. M. Frangioso, K. Isobe, D. M. Rizzo, S. I. Glassman, Mega-fire in redwood tanoak forest reduces bacterial and fungal richness and selects for pyrophilous taxa that are phylogenetically conserved. Mol Ecol 31, 2475–2493 (2022).

13. T. Whitman, et al., Soil bacterial and fungal response to wildfires in the Canadian boreal forest across a burn severity gradient. Soil Biol Biochem 138, 107571 (2019).

14. J. P. Grime, Evidence for the existence of three primary strategies in plants and its relevance to ecological and evolutionary theory. Am Nat 111, 1169–1194 (1977).

15. M. F. Pulido-Chavez, et al., Rapid bacterial and fungal successional dynamics in first year after chaparral wildfire. Mol Ecol 32, 1685–1707 (2023).

16. N. Lustenhouwer, et al., A trait-based understanding of wood decomposition by fungi. Proc Natl Acad Sci U S A 117, 11551–11558 (2020).

17. T. Camenzind, et al., Towards establishing a fungal economics spectrum in soil saprobic fungi. Nat Commun 15:1 15, 1–13 (2024).

18. J. E. Stajich, Fungal genomes and insights into the evolution of the kingdom. Microbiol Spectr 5,10.1128 (2017).

19. E. Gluck-Thaler, et al., Giant starship elements mobilize accessory genes in fungal genomes. Mol Biol Evol 39 (2022).

20. A. S. Steindorff, et al., Diversity of genomic adaptations to the post-fire environment in Pezizales fungi points to crosstalk between charcoal tolerance and sexual development. New Phytol 236, 1154–1167 (2022).

21. A. S. Steindorff, et al., Comparative genomics of pyrophilous fungi reveals a link between fire events and developmental genes. Environ Microbiol 23, 99–109 (2021).

22. I. Wapinski, A. Pfeffer, N. Friedman, A. Regev, Natural history and evolutionary principles of gene duplication in fungi. Nature 449, 54–61 (2007).

23. M. A. Ciach, J. Pawłowska, P. Górecki, A. Muszewska, The interkingdom horizontal gene transfer in 44 early diverging fungi boosted their metabolic, adaptive, and immune capabilities. Evol Lett 8, 526–538 (2024).

24. D. J. Enright, et al., Evaluating best practices for isolating pyrophilous bacteria and fungi from burned soil. bioRxiv 2024.09.16.612975 (2024).

25. M. V. Caiafa, et al., Distinct fungal and bacterial responses to fire severity and soil depth across a ten-year wildfire chronosequence in beetle-killed lodgepole pine forests. For Ecol Manage 544, 121160 (2023).

26. H. D. T. Nguyen, D. Chabot, Y. Hirooka, R. W. Roberson, K. A. Seifert, Basidioascus undulatus: Genome, origins, and sexuality. IMA Fungus 6, 215–231 (2015).

27. H. Suenaga, et al., Novel organization of aromatic degradation pathway genes in a microbial community as revealed by metagenomic analysis. ISME J 3, 1335–1348 (2009).

28. D. J. Levy-Booth, et al., Genomics and metatranscriptomics of biogeochemical cycling and degradation of lignin-derived aromatic compounds in thermal swamp sediment. The ISME J 15:3 15, 879–893 (2020).

29. A. R. Nelson, et al., Wildfire-dependent changes in soil microbiome diversity and function. Nat Microbiol 7:9 7, 1419–1430 (2022).

30. G. Fuchs, M. Boll, J. Heider, Microbial degradation of aromatic compounds — from one strategy to four. Nat Rev Microbiol 9, 803–816 (2011).

31. C. Park, J. Zhang, High expression hampers horizontal gene transfer. Genome Biol Evol 4, 523–532 (2012).

32. A. J. McCarthy, et al., Extensive horizontal gene transfer during Staphylococcus aureus co-colonization in vivo. Genome Biol Evol 6, 2697–2708 (2014).

33. B. Auxier, T. Czaran, D. K. Aanen, Modelling the consequences of the dikaryotic life cycle of mushroom-forming fungi on genomic conflict. Elife 11, e75917 (2022).

34. D. S. LeBauer, K. K. Treseder, Nitrogen limitation of net primary productivity in terrestrial ecosystems is globally distributed. Ecology 89, 371–379 (2008).

35. J. Lehmann, et al., Persistence of soil organic carbon caused by functional complexity. Nat Geosci 13, 529–534 (2020).

36. T. D. Bruns, J. A. Chung, A. A. Carver, S. I. Glassman, A simple pyrocosm for studying soil microbial response to fire reveals a rapid, massive response by Pyronema species. PLoS One 15, e0222691 (2020).

37. M. F. Pulido-Chavez, A. R. Nelson, M. J. Wilkins, S. I. Glassman, Chaparral wildfire shifts the functional potential for soil pyrogenic organic matter and nitrogen cycling. bioRxiv 2024.08.18.607989 (2024).

38. J. Houbraken, et al., Classification of Aspergillus, Penicillium, Talaromyces and related genera (Eurotiales): An overview of families, genera, subgenera, sections, series and species. Stud Mycol 95, 5–169 (2020).

39. J. B. Tanney, K. A. Seifert, Rasamsonia pulvericola sp. nov., isolated from house dust. IMA Fungus 4, 205 (2013).

40. T. K. Kolanlarlı, A. Ahsen, B. Sen, S. Ohten, Biodiversity of Penicillium species isolated from Edirne Söğütlük Forest soil (Turkey). The Journal of Fungus 10, 26–39 (2019).

41. C. F. McRae, R. D. Seppelt, A. D. Hocking, Penicillium species from terrestrial habitats in the Windmill Islands, East Antarctica, including a new species, Penicillium antarcticum. Polar Biol 21, 97–111 (1999).

42. L. W. Kong, et al., Two new antifungal indole alkaloids from an endophytic fungi Aspergillus felis obtained from cigar tobacco. Chem Nat Compd 59, 1132–1136 (2023).

43. G. Mendes, et al., Antifungal activity of extracts from Atacama Desert fungi against Paracoccidioides brasiliensis and identification of Aspergillus felis as a promising source of natural bioactive compounds. Mem Inst Oswaldo Cruz 111, 209–217 (2016).

44. X. Liu, Z. Y. Zhou, J. L. Cui, M. L. Wang, J. H. Wang, Biotransformation ability of endophytic fungi: from species evolution to industrial applications. Appl Microbiol Biotech 105, 7095–7113 (2021).

45. Y. L. Huang, M. M. N. Devan, J. M. U'Ren, S. H. Furr, A. E. Arnold, Pervasive effects of wildfire on foliar endophyte communities in montane forest trees. Microb Ecol 71, 452–468 (2016).

46. D. B. Raudabaugh, et al., Where are they hiding? Testing the body snatchers hypothesis in pyrophilous fungi. Fungal Ecol 43, 100870 (2020).

47. Y. Zhang, P. W. Crous, C. L. Schoch, K. D. Hyde, Pleosporales. Fungal Divers 53, 1–221 (2011).

48. R. Porter, et al., Degradation of polypropylene by fungi Coniochaeta hoffmannii and Pleurostoma richardsiae. Microbiol Res 277, 127507 (2023).

49. R. Riley, et al., Extensive sampling of basidiomycete genomes demonstrates inadequacy of the white-rot/brown-rot paradigm for wood decay fungi. Proc Natl Acad Sci U S A 111, 9923–9928 (2014).

50. A. R. Nelson, et al., Soil microbiome feedbacks during disturbance-driven forest ecosystem conversion. ISME J 2024, 47.

51. Z. Merényi, et al., Genomes of fungi and relatives reveal delayed loss of ancestral gene families and evolution of key fungal traits. Nat Ecol Evol 7, 1221–1231 (2023).

52. E. Shahsavari, A. Aburto-Medina, M. Taha, A. S. Ball, A quantitative PCR approach for quantification of functional genes involved in the degradation of polycyclic aromatic hydrocarbons in contaminated soils. MethodsX 3, 205 (2016).

639 53. B. Owens, Fungi borrowed bacterial gene again and again. Nature (2014).
640 https://doi.org/10.1038/NATURE.2014.15496.

641 54. Y. Wang, et al., Molecular dating of the emergence of anaerobic rumen fungi and the impact of
642 laterally acquired genes. mSystems 4, 10.1128 (2019).

643 55. D. Carter-House, J. E Stajich, S. Unruh, T. Kurbessoian, Fungal CTAB DNA Extraction v1.
644 Protocols.IO (2020). https://doi.org/10.17504/PROTOCOLS.IO.BHX8J7RW.

645 56. H. Cheng, G. T. Concepcion, X. Feng, H. Zhang, H. Li, Haplotype-resolved de novo assembly using
646 phased assembly graphs with hifiasm. Nat Methods 18, 170–175 (2021).

647 57. S. Nurk, et al., HiCanu: Accurate assembly of segmental duplications, satellites, and allelic
648 variants from high-fidelity long reads. Genome Res 30, 1291–1305 (2020).

649 58. M. Kolmogorov, J. Yuan, Y. Lin, P. A. Pevzner, Assembly of long, error-prone reads using repeat
650 graphs. Nat Biotech 37, 540–546 (2019).

651 59. A. Gurevich, V. Saveliev, N. Vyahhi, G. Tesler, QUAST: quality assessment tool for genome
652 assemblies. Bioinformatics 29, 1072–1075 (2013).

653 60. M. Manni, M. R. Berkeley, M. Seppey, E. M. Zdobnov, BUSCO: Assessing genomic data quality and
654 beyond. Curr Protoc 1, e323 (2021).

655 61. A. V. Zimin, et al., Hybrid assembly of the large and highly repetitive genome of Aegilops tauschii,
656 a progenitor of bread wheat, with the MaSuRCA mega-reads algorithm. Genome Res 27, 787–792
657 (2017).

658 62. B. Min, I. V. Grigoriev, I. G. Choi, FunGAP: Fungal genome annotation pipeline using evidence-
659 based gene model evaluation. Bioinformatics 33, 2936–2937 (2017).

660 63. P. Jones, et al., InterProScan 5: genome-scale protein function classification. Bioinformatics 30,
661 1236–1240 (2014).

662 64. K. Riehl, C. Riccio, E. A. Miska, M. Hemberg, TransposonUltimate: software for transposon
663 classification, annotation and detection. Nucleic Acids Res 50, e64–e64 (2022).

664 65. P. F. Chuckran, et al., Rapid response of nitrogen cycling gene transcription to labile carbon
665 amendments in a soil microbial community. mSystems 6, e00161-21 (2021).

666 66. T. A. Patrick, L. W. Maguire, J. Espin, C. M. Gardner, Wildfire impacts on soil microbiomes:
667 potential for disruptions to nitrogen-cycling bacteria. Environ Eng Sci 41, 337–346 (2024).

668 67. H. G. Hoang, et al., The nitrogen cycle and mitigation strategies for nitrogen loss during organic
669 waste composting: A review. Chemosphere 300, 134514 (2022).

670 68. S. A. Higgins, et al., Detection and diversity of fungal nitric oxide reductase genes (p450nor) in
671 agricultural soils. Appl Environ Microbiol 82, 2919–2928 (2016).

672 69. F. Sievers, D. G. Higgins, Clustal Omega for making accurate alignments of many protein
673 sequences. Prot Sci 27, 135–145 (2018).

70. D. M. Emms, S. Kelly, OrthoFinder: Phylogenetic orthology inference for comparative genomics. Genome Biol 20, 1–14 (2019).

71. R Core Team, R: A language and environment for statistical computing. R Foundation for Statistical Computing, Vienna, Austria (2023).

72. D. Kim, J. M. Paggi, C. Park, C. Bennett, S. L. Salzberg, Graph-based genome alignment and genotyping with HISAT2 and HISAT-genotype. Nat Biotechnol 37, 907–915 (2019).

73. R. V. Alvarez, L. S. Pongor, L. Mariño-Ramírez, D. Landsman, TPMCalculator: one-step software to quantify mRNA abundance of genomic features. Bioinformatics 35, 1960–1962 (2019).

74. Z. Zhang, et al., KaKs_Calculator: calculating Ka and Ks through model selection and model averaging. Genom Proteom Bioinform 4, 259–263 (2006).

75. J. T. Robinson, et al., Integrative genomics viewer. Nat Biotech 29, 24–26 (2011).

76. G. R. Warnes, et al., gplots: Various R programming tools for plotting data. R package version 2, 1 (2009).

77. Myles. Hollander, D. A. . Wolfe, Nonparametric statistical methods. 787 (1999).

78. M. Friendly, Corrgrams. Am Stat 56, 316–324 (2002).

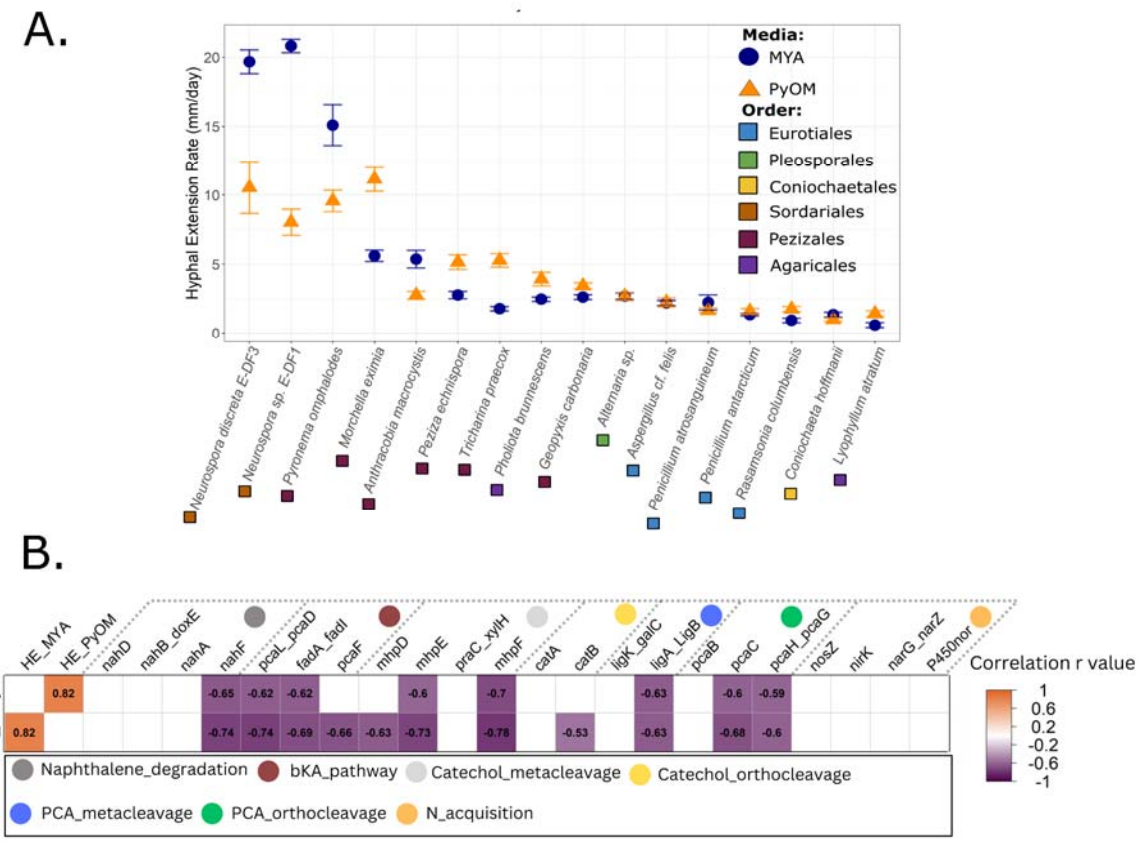

Fig 1. Hyphal extension of 16 pyrophilous fungi on Malt Yeast extract Agar (MYA) and Pyrogenic Organic Matter (PyOM) media **(A)** and pairwise Spearman's rank correlation between the hyphal extension on MYA (HE_MYA) and PyOM (HE_PyOM) media and the number of aromatic C degradation and N acquisition orthologues in each isolate **(B)**. Error bars in panel A shows standard errors of mean. Number in the cells denote pair-wise correlation r values. Gene abbreviation in panel B; nahD: 2-hydroxychromene-2-carboxylate-isomerase, nahB_doxE: cis-1,2-dihydro-1,2-dihydroxy naphthalene, nahA: Naphthalene-1,2-dioxygenase subunit-alpha, nahF: salicylaldehyde_dehydrogenase, pcaL_pcaD: 3-oxoadipate-enol-lactonase, fadA_fadI:Acetyl-Co A acyltransferase, pcaF: beta-ketoadipyl-CoA-thiolase, mhpD: 2-keto-4-pentenoate hydratase, mhpE: hydroxy_oxovalerate_aldolase, praC_xylH: 4-oxalocrotonate_tautomerase, mhpF: acetaldehyde_dehydrogenase, catA: catechol-1,2-dioxygenase, catB: muconate cycloisomerase, ligK_galC: 4-hydroxy-4-methyl-2-oxoglutarate aldolase, ligA_LigB: Protocatechuate-dioxygenase, pcaB: 3-carboxy-cis,cis-muconate-cycloisomerase, pcaC: 4-carboxy muconolactone-decarboxylase, pcaH_pcaG: Protocatechuate-3,4-dioxygenase, nosZ: nitrous-oxide-reductase, nirK: nitrite-reductase; narG_narZ: nitrate-reductase, P450nor: P450 nitric oxide reductase.

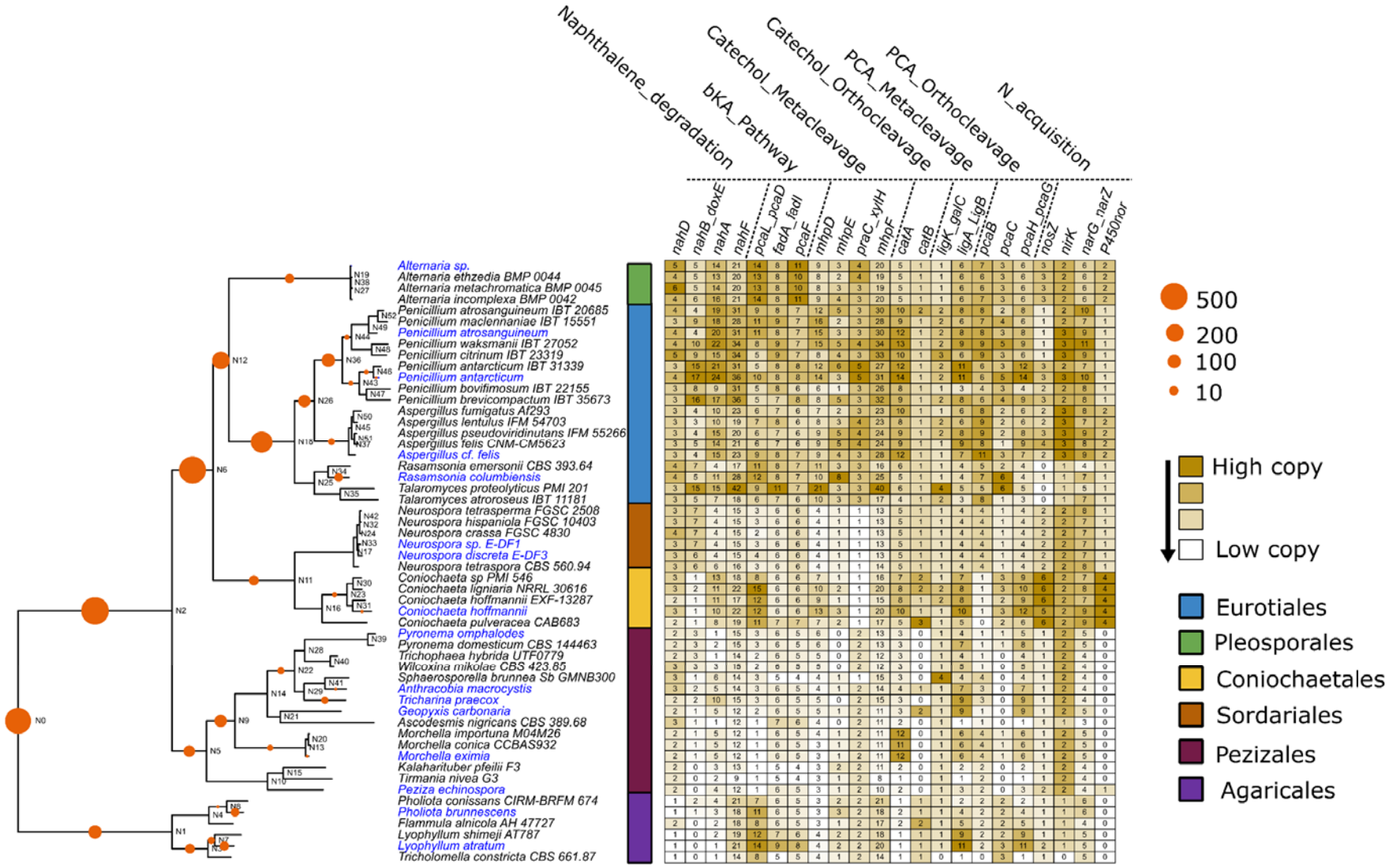
Naphthalene_degradation
bKA_Pathway
Catechol_Metacleavage
Catechol_Orthocleavage
PCA_Metacleavage
PCA_Orthocleavage
N_acquisition
nahD
nahB_doxE
nahA
nahF
pcaL_pcaD
fadA_fadI
pcaF
mhpD
mhpE
praC_xylH
mhpF
catA
catB
ligK_galC
ligA_LigB
pcaB
pcaC
pcaH_pcaG
nosZ
nirK
narG_narZ
P450nor
Alternaria sp.
Alternaria ethzedia BMP 0044
Alternaria metachromatica BMP 0045
Alternaria incomplexa BMP 0042
Penicillium atrosanguineum IBT 20685
Penicillium maclennaniae IBT 15551
Penicillium atrosanguineum
Penicillium waksmanii IBT 27052
Penicillium citrinum IBT 23319
Penicillium antarcticum IBT 31339
Penicillium antarcticum
Penicillium bovifimosum IBT 22155
Penicillium brevicompactum IBT 35673
Aspergillus fumigatus Af293
Aspergillus lentulus IFM 54703
Aspergillus pseudoviridinutans IFM 55266
Aspergillus felis CNM-CM5623
Aspergillus cf. felis
Rasamsonia emersonii CBS 393.64
Rasamsonia columbiensis
Talaromyces proteolyticus PMI 201
Talaromyces atroroseus IBT 11181
Neurospora tetrasperma FGSC 2508
Neurospora hispaniola FGSC 10403
Neurospora crassa FGSC 4830
Neurospora sp. E-DF1
Neurospora discreta E-DF3
Neurospora tetraspora CBS 560.94
Coniochaeta sp PMI 546
Coniochaeta ligniaria NRRL 30616
Coniochaeta hoffmannii EXF-13287
Coniochaeta hoffmannii
Coniochaeta pulveracea CAB683
Pyronema omphalodes
Pyronema domesticum CBS 144463
Trichophaea hybrida UTF0779
Wilcoxina mikolae CBS 423.85
Sphaerosporella brunnea Sb GMNB300
Anthracobia macrocystis
Tricharina praecox
Geopyxis carbonaria
Ascodesmis nigricans CBS 389.68
Morchella importuna M04M26
Morchella conica CCBAS932
Morchella eximia
Kalaharituber pfeilii F3
Tirmania nivea G3
Peziza echinospora
Pholiota conissans CIRM-BRFM 674
Pholiota brunnescens
Flammula alnicola AH 47727
Lyophyllum shimeji AT787
Lyophyllum atratum
Tricholomella constricta CBS 661.87
500
200
100
10
High copy
Low copy
Eurotiales
Pleosporales
Coniochaetales
Sordariales
Pezizales
Agaricales

Fig 2. Number of duplication events (orange circles on the species tree) in the aromatic carbon (C) degradation (six pathways) and nitrogen (N) acquisition orthologues in 53 genomes used for constructing orthogroups and their common ancestors vs. the total number of orthologues of 18 aromatic C degradation and four N acquisition genes. The tree leaves printed in blue are 16 pyrophilous species sequenced in this study. Gene name abbreviations: nahD: 2-hydroxychromene-2-carboxylate-isomerase, nahB_doxE: cis-1,2-dihydro-1,2-dihydroxy naphthalene, nahA: Naphthalene-1,2-dioxygenase subunit-alpha, nahF: salicylaldehyde_dehydrogenase, pcaL_pcaD: 3-oxoadipate-enol-lactonase, fadA_fadI: Acetyl-Co A acyltransferase, pcaF: beta-ketoadipyl-CoA-thiolase, mhpD: 2-keto-4-pentenoate hydratase, mhpE: hydroxy_oxovalerate_aldolase, praC_xylH: 4-oxalocrotonate_tautomerase, mhpF: acetaldehyde_dehydrogenase, catA: catechol-1,2-dioxygenase, catB: muconate cycloisomerase, ligK_galC: 4-hydroxy-4-methyl-2-oxoglutarate aldolase, ligA_LigB: Protocatechuate-dioxygenase, pcaB: 3-carboxy-cis,cis-muconate-cycloisomerase, pcaC: 4-carboxy muconolactone-decarboxylase, pcaH_pcaG: Protocatechuate-3,4-dioxygenase, nosZ: nitrous-oxide-reductase, nirK: nitrite-reductase; narG_narZ: nitrate-reductase, P450nor: P450 nitric oxide reductase.

1

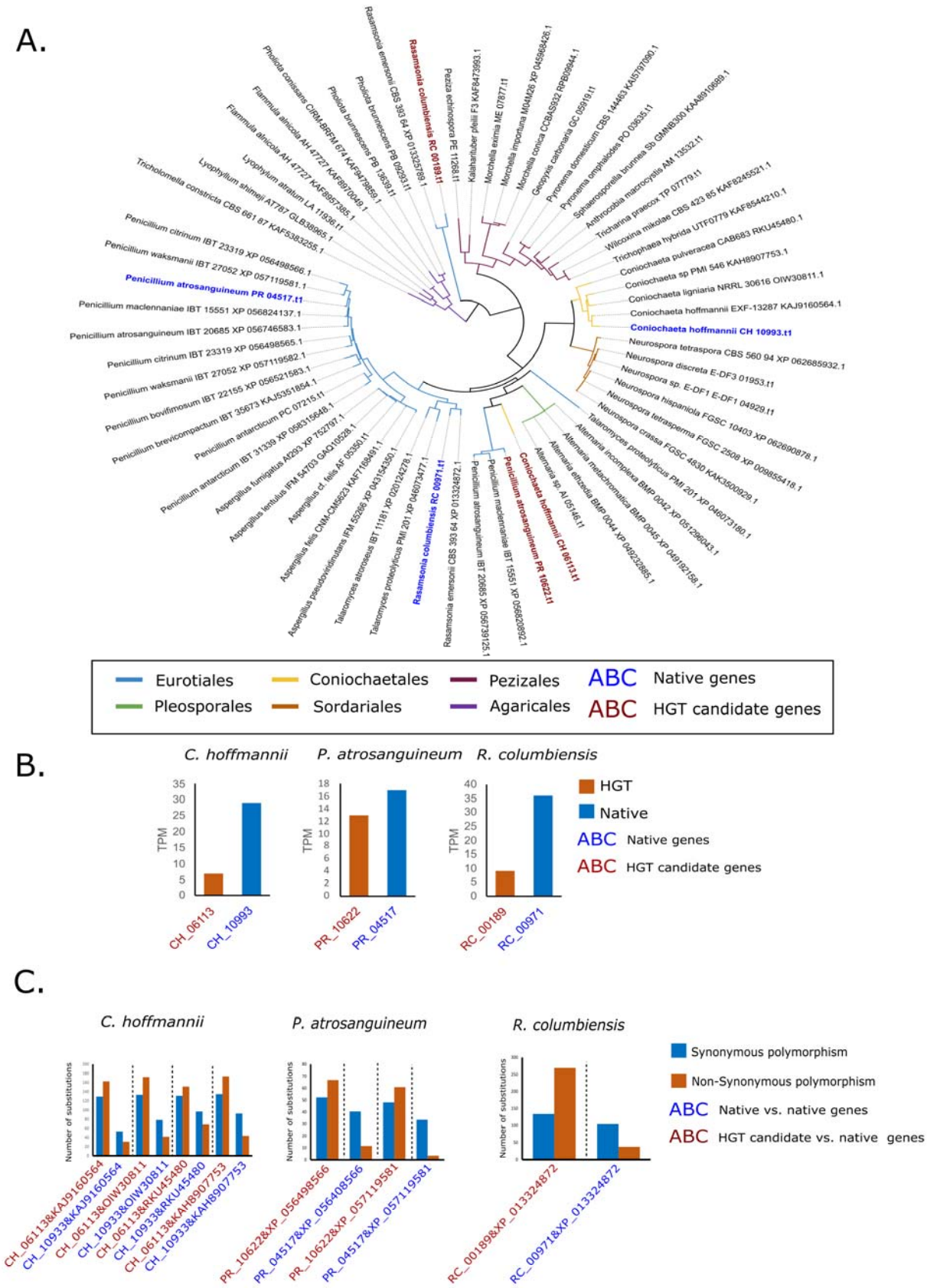
A.
Rasamsonia columbiensis RC 00189.t1
Rasamsonia emersonii CBS 393 64 XP 013325789.1
Pezizia echinospora PE 11268.t1
Kalaharituber pfeilii F3 KAF8473993.1
Morchella eximia ME 07877.t1
Morchella importuna M04M28 XP 045968426.1
Morchella conica CCBAS932 RPB09944.1
Geopyxis carbonaria GC 05919.t1
Pyronema domesticum CBS 144463 KAI5797090.1
Pyronema omphalodes PO 03635.t1
Sphaerosporella brunnea Sb GMNB300 KAA8910689.1
Anthrocobia macrocystis AM 13532.t1
Tricharina praecox TP 07779.t1
Wilcoxina mikolae CBS 423 85 KAF8245521.1
Trichophaea hybrida UTF0779 KAF8544210.1
Coniochaeta pulveracea CAB683 RKU45480.1
Coniochaeta sp PMI 546 KAH8907753.1
Coniochaeta ligniaria NRRL 30616 OIW30811.1
Coniochaeta hoffmannii EXF-13287 KAJ9160564.1
Coniochaeta hoffmannii CH 10993.t1
Neurospora tetraspora CBS 560 94 XP 062685932.1
Neurospora discreta E-DF3 01953.t1
Neurospora sp. E-DF1 E-DF1 04929.t1
Neurospora hispaniola FGSC 10403 XP 062690878.1
Neurospora tetrasperma FGSC 2508 XP 009855418.1
Neurospora crassa FGSC 4830 KAK3500929.1
Talaromyces proteolyticus PMI 201 XP 046073180.1
Alternaria incomplexa BMP 0042 XP 051296043.1
Alternaria metachromatica BMP 0045 XP 049192158.1
Alternaria ethzedia BMP 0044 XP 049232885.1
Alternaria sp. AI 05146.t1
Coniochaeta hoffmannii CH 06113.t1
Penicillium atrosanguineum PR 10622.t1
Penicillium maclennaniae IBT 15551 XP 056820892.1
Penicillium atrosanguineum IBT 20685 XP 056739125.1
Rasamsonia emersonii CBS 393 64 XP 013324872.1
Rasamsonia columbiensis RC 00971.t1
Talaromyces proteolyticus PMI 201 XP 046073477.1
Talaromyces atroroseus IBT 11181 XP 020124278.1
Aspergillus pseudoviridinutans IFM 55266 XP 043154350.1
Aspergillus felis CNM-CM5623 KAF7168491.1
Aspergillus cf. felis AF 05350.t1
Aspergillus lentulus IFM 54703 GAQ10528.1
Aspergillus fumigatus Af293 XP 752797.1
Penicillium antarcticum IBT 31339 XP 058315648.1
Penicillium antarcticum PC 07215.t1
Penicillium brevicompactum IBT 35673 KAJ5351854.1
Penicillium bovifimosum IBT 22155 XP 056521583.1
Penicillium waksmanii IBT 27052 XP 057119582.1
Penicillium citrinum IBT 23319 XP 056498565.1
Penicillium atrosanguineum IBT 20685 XP 056746583.1
Penicillium maclennaniae IBT 15551 XP 056824137.1
Penicillium atrosanguineum PR 04517.t1
Penicillium waksmanii IBT 27052 XP 057119581.1
Penicillium citrinum IBT 23319 XP 056498566.1
Tricholomella constricta CBS 661 87 KAF5383255.1
Lyophyllum shimeji AT787 GLB38965.1
Lyophylum atratum LA 11936.t1
Flammula alnicola AH 47727 KAF8957385.1
Flammula alnicola AH 47727 KAF8970049.1
Pholiota brunnescens PB 13639.t1
Pholiota brunnescens PB 09293.t1
Pholiota conissans CIRM-BRFM 674 KAF9479859.1
Eurotiales
Pleosporales
Coniochaetales
Sordariales
Pezizales
Agaricales
ABC Native genes
ABC HGT candidate genes
B.
C. hoffmannii
P. atrosanguineum
R. columbiensis
TPM
CH_06113
CH_10993
PR_10622
PR_04517
RC_00189
RC_00971
HGT
Native
ABC Native genes
ABC HGT candidate genes
C.
C. hoffmannii
P. atrosanguineum
R. columbiensis
Number of substitutions
CH_06113&KAJ9160564
CH_10933&KAJ9160564
CH_06113&OIW30811
CH_10933&OIW30811
CH_06113&RKU45480
CH_10933&RKU45480
CH_06113&KAH8907753
CH_10933&KAH8907753
PR_10622&XP_056498566
PR_04517&XP_056408566
PR_10622&XP_057119581
PR_04517&XP_057119581
RC_00189&XP_013324872
RC_00971&XP_013324872
Synonymous polymorphism
Non-Synonymous polymorphism
ABC Native vs. native genes
ABC HGT candidate vs. native genes

Fig 3. The Evidence supporting a horizontal gene transfer (HGT) event in OG0001245 orthogroup, described as catechol-1,2-dioxygenase (*catA*) in three pyrophilous species *Coniochaeta hoffmannii*, *Penicillium atrosanguineum*, and *Rasamsonia columbiensis*. Gene tree containing the 63 orthologues of OG0001245 orthogroups **(A),** the transcription (transcript per million [TPM]) values of the candidate HGT genes and their native paralogues **(B)**, and the number of synonymous and non-synonymous nucleotide polymorphisms within the candidate HGT gene and their native paralogues vs. native orthologues of sister species **(C)**.

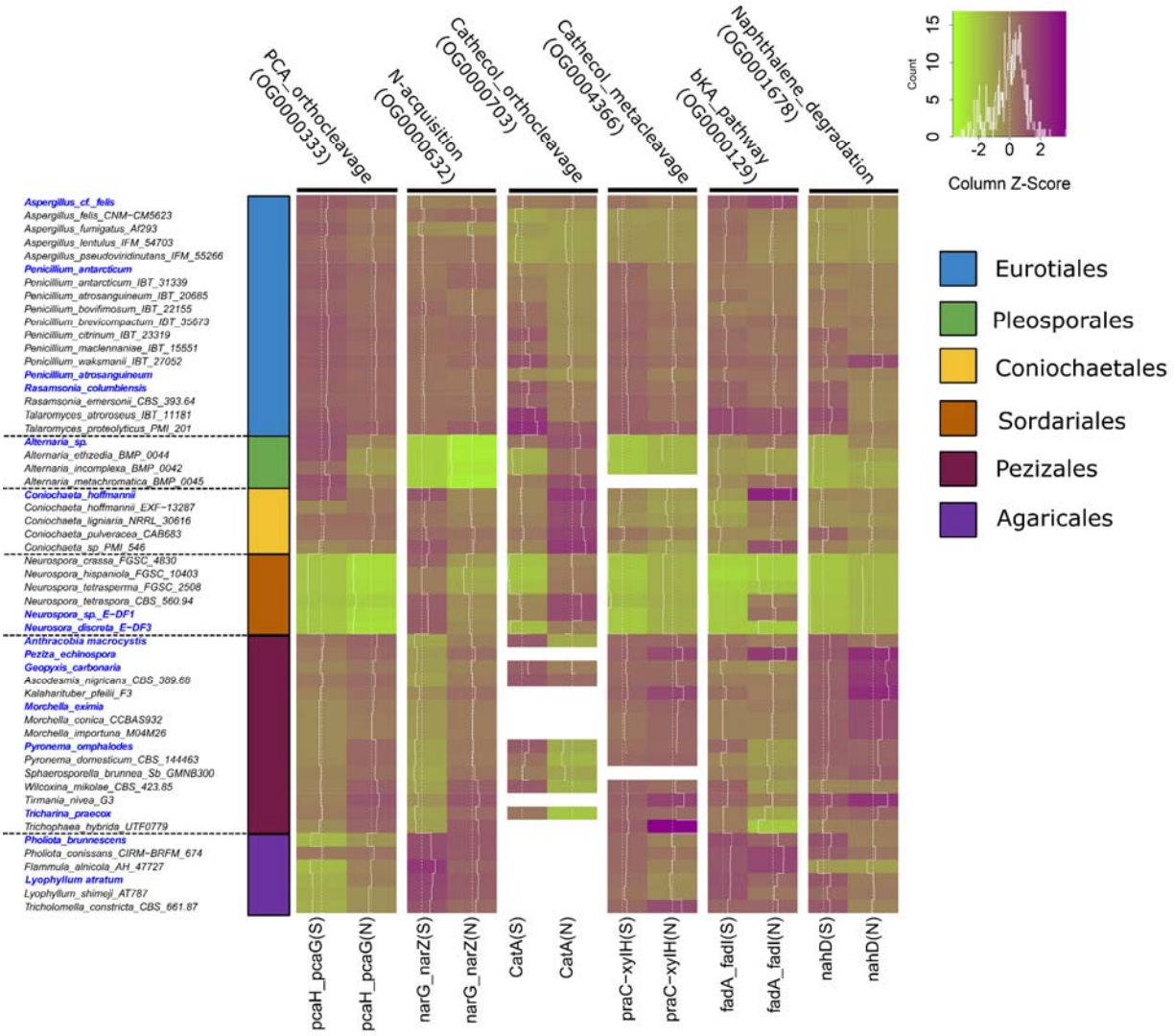

Fig 4. The number of synonymous (S) and nonsynonymous (N) nucleotide polymorphisms in six orthogroups representing five aromatic C degradation and the N acquisition pathways in 53 genomes used for orthogroup construction. Taxa in blue text were sequenced in this study. The dash line in each cell shows the median number of nucleotide polymorphisms across all taxa for each orthogroups and the solid line is that of each taxon. Orthogroups selected were described as Protocatechuate-3,4-dioxygenase (*pcaH_pcaG*), nitrate reductase (*narG-narZ*), catechol-1,2-dioxygenase (*catA*), 4-oxalocrotonate tautomerase (*praC-xylH*), Acetyl-Co A acyltransferase (*fadA_fadI*), and 2-hydroxychromene-2-carboxylate isomerase (*nahD*).